

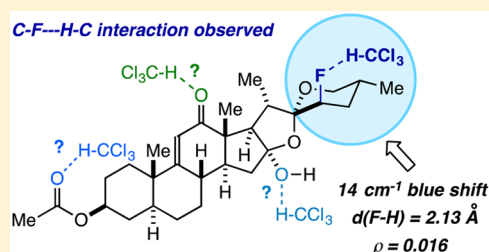
Intermolecular Aliphatic C–F...H–C Interaction in the Presence of “Stronger” Hydrogen Bond Acceptors: Crystallographic, Computational, and IR Studies

Cody Ross Pitts,[ⓑ] Maxime A. Siegler, and Thomas Lectka*

Department of Chemistry, Johns Hopkins University, 3400 North Charles Street, Baltimore, Maryland 21218, United States

S Supporting Information

ABSTRACT: An unprecedented intermolecular aliphatic C–F...H–C interaction was observed in the X-ray crystal structure of a fluorinated triterpenoid. Despite the notion of fluorine being a poor acceptor, computational and IR studies revealed this interaction to be a weak to moderate hydrogen bond with a C–H stretch vibration blue-shifted by 14 cm^{-1} and $d(\text{F}–\text{H}) = 2.13\text{ \AA}$. In addition, the aliphatic C–F bond is the preferred acceptor in the presence of multiple, traditionally *stronger* oxygen-based hydrogen bond acceptors.



The definition of “hydrogen bond” in X–H...Y interactions has evolved from the traditional (X and Y being strictly electronegative elements, for example, O and N)^{1–3} to the incorporation of such “nonclassical” interactions as C–H... π ,^{4–6} C–H...Y,^{7–9} and O–H... π .^{10,11} Today, it is widely accepted that there is a large continuum of hydrogen bonds whereby seemingly weaker or atypical interactions are encompassed, as well. Many of these nonclassical (weak) interactions are known to exert notable impacts on biological systems, catalysis, and crystal formation.¹² One of the more controversial nonclassical interactions has been the C–F...H–C hydrogen bond.^{13–16} Until recently, the role of fluorine as a hydrogen bond acceptor was debatable at best, yet well-documented intermolecular sp^2 C–F...H–C systems,¹⁷ fluoroform dimers,¹⁸ and intramolecular sp^3 C–F...H–C interactions¹⁹ have all emerged in the literature as special cases. In any event, these interactions are presumed to be weak, such that in the presence of stronger, classical acceptors such as O and N, they would be most likely disrupted.²⁰

In this note, we present a surprising occurrence whereby the fluorine atom in an aliphatic C–F bond acts as the preferred hydrogen bond acceptor in the presence of traditionally *stronger* oxygen-based acceptors (Figure 1). This C–F...H–C intermolecular interaction was discovered serendipitously in an X-ray crystal structure, studied with DFT and AIM calculations, and further characterized through IR spectroscopy as a blue-shifted weak to moderate hydrogen bond.

The parent molecule was synthesized from hecogenin acetate^{21,22} (1) in two steps: dehydrogenation using benzeneseleninic anhydride²³ followed by photochemical aliphatic C–H fluorination (Scheme 1).²⁴ The fluorination step exhibited unanticipated site-selectivity and simultaneous incorporation of a hydroxy group. Based on our previous report on enone-directed photochemical fluorination and molecular modeling, 9,11-dehydrohecogenin acetate does not appear to

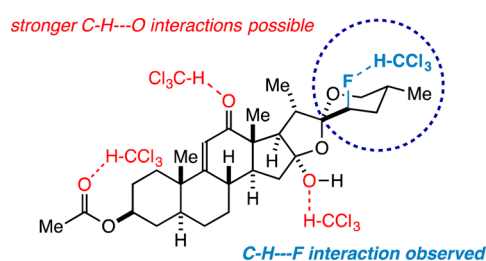


Figure 1. C–F...H–C interaction observed in the presence of traditionally stronger oxygen-based hydrogen bond acceptors.

be poised for so-called mode I, II, III, or IV fluorination.²⁴ Instead, we imagine that this “frustrated” excited-state enone participates in intermolecular hydrogen atom abstraction. However, the mechanism for this transformation and rationale for site-selectivity/oxygen incorporation are not yet understood and beyond the scope of this study. In any case, the major diastereomer **2** was isolated, crystallized from a mixture of chloroform and hexanes using a solvent evaporation technique, and subjected to single-crystal X-ray diffraction. We found that the composition of the crystal was 1:1 parent molecule 2:CHCl₃ with a well-ordered solvent molecule located in proximity to the C–F bond (Figure 2). Surprisingly, the spatial orientation of chloroform and the experimental F–C² distance of 3.14 Å in the crystal structure indicated a significant C–F...H–C interaction (Table 1).

Through DFT calculations, an average F...H distance of 2.13 Å was determined with four different functionals using fixed heavy atom coordinates from the crystal structure (Table 1). Although this distance is greater than previously reported forced intramolecular aliphatic C–F...H–C interactions (e.g.,

Received: February 2, 2017

Published: February 27, 2017

Scheme 1. Synthesis of the Parent Molecule 2 (Major Diastereomer Depicted with Respect to the C–F Bond)

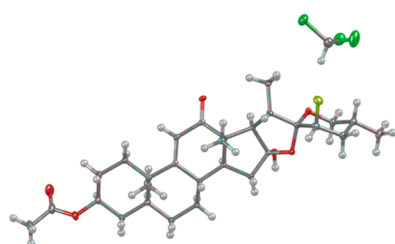
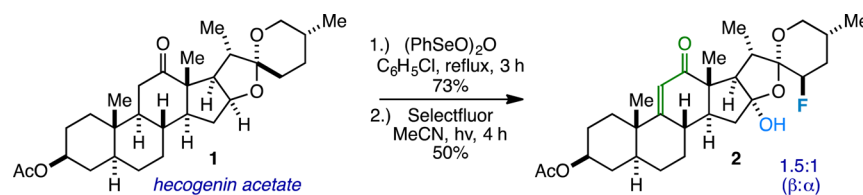


Figure 2. Crystal structure determined from single-crystal X-ray diffraction (displacement ellipsoids given at 50% probability level) with hydrogen atoms refined using a riding model.

1.83–1.91 Å),¹⁹ to our knowledge, it is among the shortest *intermolecular* contacts of this type to date.²⁵ Additionally, this interaction is less frequently observed with aliphatic C–F bonds than sp² C–F, sp C–F, or perfluorinated acceptors.^{26–30} One might argue that chloroform and the alkyl fluoride are forced into close proximity unfavorably due to crystal packing. However, we also performed full geometry optimizations on the parent molecule 2:CHCl₃ complex (unfixed CHCl₃) with the same functionals/basis sets and found average F...H distances of 2.14 Å (ranging 2.09–2.20 Å) and F–C² distances of 3.21 Å (ranging 3.15–3.28 Å). The fact that the free chloroform molecule was not repelled from the parent compound, but instead maintained atomic distances and angles similar to that of the crystal structure, implies an energetic minimum whereby an attractive F...H interaction does exist.

Can we consider this a hydrogen bond? The basic criterion of a covalently bound hydrogen atom being at the center of the two species is in place, but by the most prudent definition, we must consider (1) the stabilization of the complex relative to the individual species and (2) the nature of charge transfer from the acceptor to the donor.³¹ For one, straightforward DFT

calculations of the interaction energy predict the complex to be 4.50–4.84 kcal/mol more stable than the individual non-hydrogen-bonded entities (Table 1). On the vast energy continuum of hydrogen bonding, this could be indicative of a weak to moderate hydrogen bonding interaction.³² Regarding the nature of the *bond* in this attractive interaction, electron density (ρ) calculations using the atoms-in-molecules (AIM) program provide more insight.³³ One of the criteria used to assess bonding is the presence of a bond critical point (BCP).³⁴ According to the AIM calculations, a BCP between the fluorine and hydrogen atom exists with $\rho = 0.016$ with the proper Laplacian of electron density being consistent with a weak to moderate hydrogen bond.^{32,35} With respect to the nature of charge transfer, a natural bond orbital (NBO) analysis is informative. As anticipated, we found an increase in net charge of the hydrogen atom in the calculated complex versus free chloroform (positive Δq_H); this is at the expense of the net charge of the fluorine acceptor (negative Δq_F).³⁶

Beyond the above quantum mechanical analyses, the complex was studied using solid-state IR spectroscopy, as frequency shifts are often correlated with the strength of a hydrogen bonding interaction. IR data were obtained on the crystal using an ATR-IR instrument, as solution-phase analyses do not discriminate C–F...H–C interactions among other possible hydrogen bonds in this system. The weak Cl₃C–H stretch was difficult to analyze in the presence of a broad O–H stretch; consequently, another crystal was grown from a mixture of deuterated chloroform (CDCl₃) and hexanes to study a more distinguishable Cl₃C–D stretch in the complex.³⁷ An IR spectrum revealed the incorporation of CDCl₃ in the crystal and furthermore exhibited an *increase* in C–D stretch vibration frequency (relative to CDCl₃) by 14 cm^{–1} (Figure 3). Single-crystal X-ray crystallography confirmed that this sample is, in fact, the same polymorph with 1:1 parent molecule

Table 1. DFT and AIM Computational Analyses

functional/basis set	$d(\text{F}–\text{H})$ (Å) ^a	$d(\text{F}–\text{C}^2)$ (Å)	$\theta_{\text{Cl}–\text{F}–\text{H}}$	$\phi_{\text{F}–\text{H}–\text{C}^2}$	ρ (10 ^{–2}) ^b	ΔE_{int} (kcal/mol) ^c	Δq_{H} ^d	Δq_{F} ^d
B3LYP/6-311++G**	2.13	3.20	140.4	170.4		–4.84	0.028	–0.018
B3PW91/6-311++G**	2.20	3.28	160.2	174.7		–4.52	0.026	–0.016
PBEPBE/6-311++G**	2.13	3.21	137.5	171.8		–4.63	0.026	–0.018
CAM-B3LYP/6-311++G**	2.09	3.15	142.1	166.1	1.6	–4.50	0.029	–0.018

^aHydrogen atom on chloroform is in a calculated position based on a fully optimized structure (no bond constraints). ^bRefers to electron density at BCP. ^cInteraction energy, calculated as $\Delta E_{\text{int}} = E(2:\text{CHCl}_3) - [E(2) + E(\text{CHCl}_3)]$. ^dChange in natural charge of the specified atom in the hydrogen-bonded complex relative to the individual species by NBO analysis.

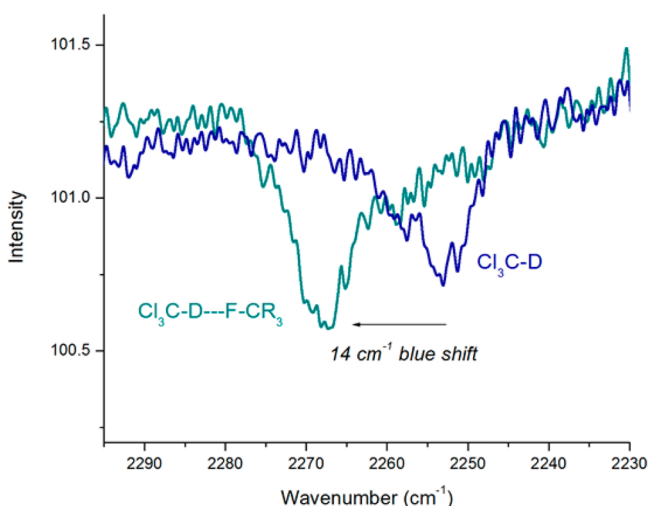


Figure 3. Zoomed-in overlay of the IR spectra of the 1:1 parent molecule 2:CDCl₃ crystal and pure CDCl₃, highlighting the blue shift in the C–D stretch vibration frequency.

2:CDCl₃ incorporation. Thus, this frequency shift is attributed to the corresponding C–F···D–C interaction. Conventionally, an X–H···Y interaction manifests in a weakening of the X–H bond and thus bond elongation and a decrease (or red shift) in the X–H stretch vibration frequency.³⁸ Yet, this particular C–H···F interaction experiences a less common *blue shift*.³⁹ Such an interaction has been noted in many instances as an “improper” hydrogen bond, as it harbors the appropriate stabilizing features but manifests in X–H bond compression.³¹

What is more, this blue shift is predicted by DFT calculations. Vibrational analyses of the isotopomers using the CAM-B3LYP/6-311+G** method suggest an 11 cm⁻¹ shift in the fully optimized structure of the complex and a 13 cm⁻¹ shift in the calculated structure with fixed chloroform coordinates. The calculations were also conducted using the various functionals in Table 1; in each case, a blue shift was determined.

Perhaps, the most intriguing aspect is not only that this C–F···H–C blue-shifted hydrogen bonding interaction exists, rather that it exists in the presence of stronger oxygen-based hydrogen bonding acceptors. When chloroform was placed near a number of available oxygen atoms on the parent molecule, several structures were optimized at B3LYP/6-311+G** that also suggest potential hydrogen bonding interactions. Naturally, when the energies of these systems are compared to the energy of the F-bound chloroform, the calculated O-bound chloroform structures are consistently lower in energy by 1.26–2.15 kcal/mol (Figure 4).^{20,40} So why is the C–F···H–C interaction occurring instead? In short, the crystal packing arrangement with the C–F···H–C interaction is

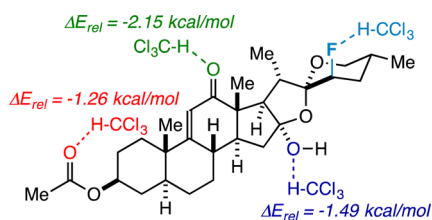


Figure 4. Relative energies of O-bound chloroform complexes to the observed F-bound chloroform complex, calculated at B3LYP/6-311+G**.

the most favorable.⁴¹ It is extremely difficult to model alternative packing scenarios, but we can note some important features from the packing diagram at hand. For one, the chlorine atoms do not have any significant short contacts with other atoms in the lattice; therefore, the presence and orientation of chloroform must be influenced primarily by the C–F···H–C interaction. Additionally, if we consider other interactions, the diagram contains an intermolecular O–H···O=C interaction ($d(\text{H–O}) = 1.98 \text{ \AA}$) between the hydroxy group and the enone oxygen that is certainly influencing the arrangement. It is possible that this conventionally stronger O–H···O hydrogen bonding interaction precludes a C–H···O interaction at this site, but in any case, the C–H···F interaction evidently plays an important role in crystal packing.

In all, we find the intermolecular aliphatic C–F···H–C hydrogen bonding interaction to be a surprising and notable result. By probing this phenomenon with DFT and AIM calculations, we have found that the interaction meets the basic criteria for a hydrogen bond. Additionally, the X-ray crystal structure and computational data are substantiated through spectroscopic (IR) evaluation of the complex that determines a blue shift of ca. 14 cm⁻¹, indicative of a rarer hydrogen bond characterized by C–H bond compression. While other features of the crystal packing undoubtedly influence its occurrence, the fact that the C–H···F interaction is preferred over a packing arrangement with a more favorable C–H···O interaction (or no chloroform incorporation) is significant. Given the biological relevance of similar triterpenoids, this result may prompt investigation of aliphatic fluorine interactions, for instance, in enzyme active sites.

EXPERIMENTAL SECTION

General Methods. Unless otherwise stated, all reactions were carried out under strictly anhydrous conditions and N₂ atmosphere. Solvents were dried and distilled by standard methods. All ¹H and ¹³C spectra were acquired on a 400 MHz NMR spectrometer in CDCl₃, and ¹⁹F spectra were acquired on a 300 MHz NMR spectrometer in CD₃CN or CDCl₃. The ¹H, ¹³C, and ¹⁹F NMR chemical shifts are given in parts per million (δ) with respect to an internal tetramethylsilane (TMS, $\delta = 0.00 \text{ ppm}$) standard and/or 3-chlorobenzotrifluoride ($\delta = -64.2 \text{ ppm}$ relative to CFCl₃).⁴² NMR data are reported in the following format: chemical shift [integration, multiplicity (s = singlet, d = doublet, t = triplet, q = quartet, m = multiplet), coupling constants (Hz)]. IR data were obtained using an ATR-IR instrument or FT-IR with a flat CaF₂ cell. All analyses were completed using positive ion mode electrospray ionization (Apollo II ion source) on a Bruker 12.0 T APEX-Qe FTICR-MS. Spectral data were processed with Bruker software. Photochemical reactions were run in a Rayonet reactor using 300 nm bulbs. The Gaussian 09 package was used for DFT calculations.⁴³

Compound Characterization. *9,11-Dehydrohecogenin Acetate.* Hecogenin acetate **1** (1.4 g, 2.9 mmol) and benzeneseleninic acid anhydride (2.1 g, 5.8 mmol) were added to a flame-dried three-neck round-bottom flask equipped with a stir bar and reflux condenser under N₂. Anhydrous chlorobenzene (12 mL) was added via syringe, and the reaction mixture was stirred and heated to reflux for 3 h. The reaction mixture was quenched with saturated aqueous NaHCO₃ and transferred to a separatory funnel. The crude mixture was extracted into EtOAc, and the combined organic layers were washed with H₂O and brine. The crude mixture was dried with MgSO₄, filtered through Celite, and concentrated. The crude residue was purified via gradient column chromatography on silica gel eluting with 10:90 to 20:80 EtOAc/hexanes to provide 9,11-dehydrohecogenin acetate as a pale white solid (1.0 g, 73% yield): mp = 213–215 °C; ¹H NMR (CDCl₃) δ 5.65 (1H, d, $J = 2.0 \text{ Hz}$), 4.67–4.59 (1H, m), 4.38–4.32 (1H, m), 3.43 (1H, ddd, $J = 10.8, 4.2, 2.0 \text{ Hz}$), 3.31 (1H, t, $J = 11.0 \text{ Hz}$), 2.51–

2.44 (1H, m), 2.35 (1H, dd, $J = 8.8, 7.2$ Hz), 2.18–2.12 (1H, m), 2.02–1.89 (2H, m), 1.99 (3H, s), 1.82–1.33 (16H, m), 1.09–1.02 (7H, m), 0.88 (3H, s), 0.75 (3H, d, $J = 6.4$ Hz); $^{13}\text{C}\{^1\text{H}\}$ NMR (CDCl_3) δ 204.6, 170.4, 170.3, 119.9, 109.2, 79.6, 72.5, 66.8, 53.6, 52.2, 50.9, 42.4, 42.3, 39.1, 36.7, 34.4, 33.6, 32.3, 31.3, 31.2, 30.1, 28.7, 27.4, 27.1, 21.2, 18.3, 17.0, 14.9, 13.0; ν_{max} (CaF_2 , CHCl_3) 1726, 1669 cm^{-1} ; HRMS (ESI/ion-trap) m/z $[\text{M} + \text{Na}]^+$ calcd for $\text{C}_{29}\text{H}_{42}\text{O}_5\text{Na}^+$ 493.2925, found 493.2900.

23 β -Fluoro-16 α -hydroxy-9,11-dehydrohecogenin Acetate (2). Selectfluor (195 mg, 0.55 mmol) and 9,11-dehydrohecogenin acetate (118 mg, 0.25 mmol) were added to an oven-dried μO vial equipped with a stir bar; the vial was then sealed with a cap with septum using a crimper and evacuated/refilled with N_2 multiple times. Anhydrous CH_3CN (6.0 mL) was added, and the reaction mixture was irradiated at 300 nm in a Rayonet reactor while being stirred. After 4 h, an aliquot was taken for ^{19}F NMR analysis. The reaction mixture was then poured over Et_2O , filtered through Celite, and concentrated. The crude reaction mixture was purified via gradient column chromatography on silica gel eluting with EtOAc /hexanes to provide **2** as a white solid (40 mg, 32% yield): mp = 196–198 $^\circ\text{C}$; ^1H NMR (CDCl_3) δ 5.71 (1H, d, $J = 2.0$ Hz), 4.70–4.62 (1H, m), 4.34 (1H, dm, $J = 47.5$ Hz), 3.66–3.54 (2H, m), 3.35 (1H, br s), 2.50–2.43 (1H, m), 2.36 (1H, d, $J = 6.8$ Hz), 2.25 (1H, quint, $J = 6.9$ Hz), 2.20–2.11 (1H, m), 2.09–2.05 (2H, m), 2.01 (3H, s), 2.00–1.92 (3H, m), 1.79–1.73 (3H, m), 1.71–1.40 (7H, m), 1.25 (3H, dd, $J = 6.9, 0.7$ Hz), 1.22–1.12 (1H, m), 1.08 (3H, s), 0.90 (3H, s), 0.82 (3H, d, $J = 6.7$ Hz); $^{13}\text{C}\{^1\text{H}\}$ NMR (CDCl_3) δ 203.7, 170.7, 170.5, 119.8, 115.8, 108.0 (d, $J = 26.2$ Hz), 89.9 (d, $J = 172.9$ Hz), 72.5, 67.5, 63.4, 52.3, 51.4, 42.4, 42.0, 39.3, 38.2, 36.5, 34.4, 34.1 (d, $J = 20.3$ Hz), 33.7, 32.2, 27.4, 27.2, 24.0, 21.3, 18.3, 16.5, 14.5, 13.9; ^{19}F NMR (CDCl_3) δ -194.0 (1F, m); ν_{max} (CaF_2 , CHCl_3) 3560 (br), 1728, 1674 cm^{-1} .

X-ray Data for 2:CHCl₃: $F_w = 623.98$, colorless thick plate, $0.68 \times 0.43 \times 0.12$ mm, orthorhombic, $P2_12_12_1$ (no. 19), $a = 6.62124(7)$ Å, $b = 13.29651(13)$ Å, $c = 34.1798(4)$ Å, $V = 3009.17(6)$ Å³, $Z = 4$, $D_x = 1.377$ g cm^{-3} , $\mu = 3.159$ mm⁻¹, $T_{\text{min}} - T_{\text{max}} = 0.295 - 0.719$; 19 696 reflections were measured up to a resolution of $(\sin \theta/\lambda)_{\text{max}} = 0.62$ Å⁻¹; 5910 reflections were unique ($R_{\text{int}} = 0.0259$), of which 5798 were observed [$I > 2\sigma(I)$]; 367 parameters were refined; $R1/wR2$ [$I > 2\sigma(I)$] 0.0353/0.1003; $R1/wR2$ [all refln] 0.0359/0.1009; $S = 1.092$. Residual electron density found between -0.45 and 0.65 e Å⁻³.

ASSOCIATED CONTENT

Supporting Information

The Supporting Information is available free of charge on the ACS Publications website at DOI: 10.1021/acs.joc.7b00268.

X-ray crystallographic specifications, NMR spectra, and computational data (PDF)

X-ray data for 2:CHCl₃ (CIF)

AUTHOR INFORMATION

Corresponding Author

*E-mail: lectka@jhu.edu.

ORCID

Cody Ross Pitts: 0000-0003-1047-8924

Notes

The authors declare no competing financial interest.

ACKNOWLEDGMENTS

T.L. thanks the National Science Foundation (NSF) (CHE-1465131) for support. C.R.P. thanks Johns Hopkins for a Glen E. Meyer '39 Fellowship. The authors also thank COSMIC Lab (Old Dominion University) for their assistance.

REFERENCES

(1) Pauling, L. *The Nature of the Chemical Bond*, 3rd ed.; Cornell University Press: New York, 1960.

(2) Jeffrey, G. A. *An Introduction to Hydrogen Bonding*; Oxford University Press: New York, 1997.

(3) Arunan, E.; Desiraju, G. R.; Klein, R. A.; Sadlej, J.; Scheiner, S.; Alkorta, I.; Clary, D. C.; Crabtree, R. H.; Dannenberg, J. J.; Hobza, P.; Kjaergaard, H. G.; Legon, A. C.; Mennucci, B.; Nesbitt, D. J. *Pure Appl. Chem.* **2011**, *83*, 1637–1641.

(4) Steiner, T.; Starikov, E. B.; Amado, A. M.; Teixeira-Dias, J. J. C. *J. Chem. Soc., Perkin Trans. 2* **1995**, 1321–1326.

(5) Steiner, T.; Tamm, M.; Grzegorzewski, A.; Schulte, M.; Veldman, N.; Schreurs, A. M. M.; Kanters, J. A.; Kroon, J.; van der Maas, J.; Lutz, B. *J. Chem. Soc., Perkin Trans. 2* **1996**, 2441–2446.

(6) Sodupe, M.; Rios, R.; Branchadell, V.; Nicholas, T.; Oliva, A.; Dannenberg, J. J. *J. Am. Chem. Soc.* **1997**, *119*, 4232–4238.

(7) Legon, A. C.; Roberts, B. P.; Wallwork, A. L. *Chem. Phys. Lett.* **1990**, *173*, 107–114.

(8) Legon, A. C.; Wallwork, A. L.; Warner, H. E. *Chem. Phys. Lett.* **1992**, *191*, 98–101.

(9) Steiner, T.; Desiraju, G. R. *Chem. Commun.* **1998**, 891–892.

(10) Tarakeshwar, P.; Kim, K. S.; Brutschy, B. *J. Chem. Phys.* **2000**, *112*, 1769–1781.

(11) Struble, M. D.; Holl, M. G.; Coombs, G.; Siegler, M. A.; Lectka, T. *J. Org. Chem.* **2015**, *80*, 4803–4807.

(12) Takahashi, O.; Kohno, Y.; Nishio, M. *Chem. Rev.* **2010**, *110*, 6049–6076.

(13) Desiraju, G. R.; Steiner, T. *The Weak Hydrogen Bond in Structural Chemistry and Biology*; Oxford University Press: Oxford, UK, 1999; pp 205–209.

(14) Howard, J. A. K.; Hoy, V. J.; O'Hagan, D.; Smith, G. T. *Tetrahedron* **1996**, *52*, 12613–12622.

(15) Schneider, H.-J. *Chem. Sci.* **2012**, *3*, 1381–1394.

(16) Champagne, P. A.; Desroches, J.; Paquin, J.-F. *Synthesis* **2015**, *47*, 306–322.

(17) Thakur, T. S.; Kirchner, M. T.; Bläser, D.; Boese, R.; Desiraju, G. R. *CrystEngComm* **2010**, *12*, 2079–2085.

(18) Kryachko, E.; Scheiner, S. *J. Phys. Chem. A* **2004**, *108*, 2527–2535.

(19) Struble, M. D.; Strull, J.; Patel, K.; Siegler, M. A.; Lectka, T. *J. Org. Chem.* **2014**, *79*, 1–6.

(20) Shimoni, L.; Glusker, J. P. *Struct. Chem.* **1994**, *5*, 383–397.

(21) Corbiere, C.; Liagre, B.; Bianchi, A.; Bordji, K.; Dauça, M.; Netter, P.; Beneytout, J. L. *Int. J. Oncol.* **2003**, *22*, 899–905.

(22) Santos Cerqueira, G.; dos Santos e Silva, G.; Rios Vasconcelos, E.; Fragoso de Freitas, A. P.; Arcanjo Moura, B.; Silveira Macedo, D.; Lopes Souto, A.; Barbosa Filho, J. M.; de Almeida Leal, L. K.; de Castro Brito, G. A.; Souccar, C.; de Barros Viana, G. S. *Eur. J. Pharmacol.* **2012**, *683*, 260–269.

(23) Barton, D. H. R.; Lester, D. J.; Ley, S. V. *J. Chem. Soc., Perkin Trans. 1* **1980**, 2209–2212.

(24) Pitts, C. R.; Bume, D. D.; Harry, S. A.; Siegler, M. A.; Lectka, T. *J. Am. Chem. Soc.* **2017**, *139*, 2208–2211.

(25) A CSD search (CSD version 5.37 + 1 update Feb 2016) was performed to check for C–F...H–CCl₃ intermolecular interactions. Here, 109 hits were found, and the H...F distances ranged from 2.25 to 2.67 Å. Most of the C–F bonds are from aryl fluorides and trifluoromethyl groups.

(26) Dikundwar, A. G.; Sathishkumar, R.; Guru Row, T. N. Z. *Kristallogr. - Cryst. Mater.* **2014**, *229*, 609–624.

(27) Shukla, R.; Chopra, D. *CrystEngComm* **2015**, *17*, 3596–3609.

(28) Omorodion, H.; Twamley, B.; Platts, J. A.; Baker, R. J. *Cryst. Growth Des.* **2015**, *15*, 2835–2841.

(29) Taylor, R. *Cryst. Growth Des.* **2016**, *16*, 4165–4168.

(30) Panini, P.; Gonnade, R. G.; Chopra, D. *New J. Chem.* **2016**, *40*, 4981–5001.

(31) Hobza, P.; Havlas, Z. *Chem. Rev.* **2000**, *100*, 4253–4264.

(32) Parthasarathi, R.; Subramanian, V.; Sathyamurthy, N. *J. Phys. Chem. A* **2006**, *110*, 3349–3351.

(33) Keith, T. A. *AIMAll*, version 13.05.06; TK Gristmill Software, Overland Park KS, 2013 (aim.tkgristmill.com).

(34) Bader, R. F. W. *Acc. Chem. Res.* **1985**, *18*, 9–15.

- (35) Grabowski, S. J. *J. Phys. Chem. A* **2011**, *115*, 12789–12799.
- (36) Charge transfer from the proton acceptor to the proton donor is a common feature in nearly all hydrogen bonding definitions. For example, see: Popelier, P. L. A. *J. Phys. Chem. A* **1998**, *102*, 1873–1878.
- (37) Anslyn, E. V.; Dougherty, D. A. *Modern Physical Organic Chemistry*; University Science Books: Sausalito, CA, 2006.
- (38) Scheiner, S. *Hydrogen Bonding*; Oxford University Press: New York, 1997.
- (39) For another example of blue-shifted hydrogen bonding in a haloform complex, see: Van den Kerkhof, T.; Bouwen, A.; Goovaerts, E.; Herrebout, W. A.; van der Veken, B. J. *J. Phys. Chem. Chem. Phys.* **2004**, *6*, 358–362.
- (40) For examples of C–H···O hydrogen bonding in crystals, see: Desiraju, G. R. *Acc. Chem. Res.* **1991**, *24*, 290–296.
- (41) Dauber, P.; Hagler, A. T. *Acc. Chem. Res.* **1980**, *13*, 105–112.
- (42) Naumann, D.; Kischkewitz, J. J. *Fluorine Chem.* **1990**, *47*, 283–299.
- (43) Huczynski, A.; Rutkowski, J.; Brzezinski, B. *Struct. Chem.* **2011**, *22*, 627–634.
- (44) Determined for the 2:CHCl₃ crystal.